photonics

MDPI

Article

Experimental Study on the In-Band Amplified Spontaneous Emission in the Single-Mode Continuous-Wave Yb-Doped Fiber Amplifier Operating near 980 nm

Zhaode Li [1,2,3,†], Shangde Zhou [1,2,3,†], Aimin Liu [1,2,3], Jianqiu Cao [1,2,3,*], Zhihe Huang [1,2,3] and Jinbao Chen [1,2,3]

[1] College of Advanced Interdisciplinary Studies, National University of Defense Technology, Changsha 410073, China; zhaodeli0038@nudt.edu.cn (Z.L.); zhoushangde18@nudt.edu.cn (S.Z.); liuaimin@nudt.edu.cn (A.L.); huangzhihe@nudt.edu.cn (Z.H.); chenjinbao@nudt.edu.cn (J.C.)
[2] State Key Laboratory of Pulsed Power Laser Technology, Changsha 410073, China
[3] Hunan Provincial Key Laboratory of High Energy Laser Technology, Changsha 410073, China
* Correspondence: caojianqiu@nudt.edu.cn
† These authors contributed equally to this work.

Abstract: In this paper, the in-band amplified spontaneous emission (ASE) in the Yb-doped continuous-wave (CW) fiber amplifier operating near 980 nm is experimentally studied for the first time, to the best of our knowledge. A core-pumped single-mode Yb-doped fiber amplifier is fabricated and the effects of pump power, seed power, and active fiber length on the in-band ASE are investigated in the experiment. It is found that a strong in-band ASE around 980 nm can be observed even with no obvious ASE around 1030 nm present. It is also found that with the increment of pump power, the in-band ASE can be enhanced faster than the signal light. By studying the effects of seed power and active fiber length, it is found that, although increasing the seed power and shortening the active fiber can both suppress the in-band ASE, the latter method is less effective than the former one. The theoretical study is also carried out in order to understand the difference between the in-band ASE and 1030-nm ASE. The experimental observations are also discussed qualitatively with the theoretical results. We believe that the pertinent results and discussions can provide significant guidance for understanding the in-band ASE in the Yb-doped fiber amplifier operating near 980 nm.

Keywords: fiber amplifier; Yb-doped fiber; amplified spontaneous emission

check for updates

Citation: Li, Z.; Zhou, S.; Liu, A.; Cao, J.; Huang, Z.; Chen, J. Experimental Study on the In-Band Amplified Spontaneous Emission in the Single-Mode Continuous-Wave Yb-Doped Fiber Amplifier Operating near 980 nm. *Photonics* **2022**, *9*, 377. https://doi.org/10.3390/photonics9060377

Received: 28 April 2022
Accepted: 23 May 2022
Published: 26 May 2022

1. Introduction

The Yb-doped fiber laser has attracted much attention because of its wide applications in the fields of industrial cutting, material processing, optical communication, and so on. In last two decades, the Yb-doped fiber experienced a rapid development [1–5], and a 20-kW single-mode fiber laser has been demonstrated [5]. Nowadays, the majority of pertinent studies are focused on wavelengths larger than 1 μm, within the band of which, the gain of a Yb-doped fiber can be most conveniently obtained [3]. However, besides the band larger than 1 um, the Yb-doped fiber can also be utilized to generate an emission near 980 nm. In recent years, the Yb-doped fiber laser operating near 980 nm also developed rapidly, and has the advantages of high brightness, compactness, stability, and so on. It can not only be applied as the high-brightness pump source for power up-scaling of Yb/Er-doped fiber lasers [3,4], but can also be applied for pumping ultrafast solid-state and fiber lasers. Furthermore, by means of frequency doubling and tripling, it can also be applied for generating blue-green and ultraviolet emissions [6,7]. Therefore, the Yb-doped fiber laser operating near 980 nm is becoming more and more attractive.

One well-known challenge for achieving high-power lasing around 980 nm is the ASE around 1030 nm [8–11]. The reason is that lasing around 980 nm is produced by the three-level transmission of Yb-ions, while the ASE around 1030 nm is produced by the four-level transmission of -Yb-ions. As a result, the ASE around 1030 nm has a lower pump threshold and can be amplified more easily than lasing around 980 nm, and their gain competition then becomes unavoidable. The issue of how to suppress the ASE around 1030 nm is considered a key in the designation of the fiber laser and amplifier around 980 nm.

Nowadays, the most widely used method to suppress the ASE around 1030 nm is increasing the core-to-cladding ratio of the Yb-doped fiber [8]. A number of studies have focused on the design of the Yb-doped fiber. In 2008, by using a large-core Yb-doped photonic crystal fiber (PCF) (with core/cladding diameter of 80/200 μm), a 100-W level 977-nm Yb-doped fiber oscillator was demonstrated with the 1030-nm ASE well suppressed [12]. In 2019, by enlarging the loss of the 1030-nm ASE with the photonic bandgap fiber (PBGF), a 151-W 978-nm all-fiber oscillator was demonstrated [13].

Besides the fiber oscillator, the fiber amplifier operating near 980 nm is also attractive because of its important role in the power up-scaling of 980-nm lasing [14–24]. In recent years, the high-power fiber amplifier has rapidly developed, and the kilo-Watt all-fiber amplifier has been demonstrated with the large-core Yb-doped fiber [19]. However, different from the case of the fiber oscillator, it was found that the in-band ASE around 980 nm can be more serious than the 1030-nm ASE in the high-power fiber amplifier, and can become the key limitation of power up-scaling [19,20]. Additionally, with the amplified noise, such ASE will also do harm to applications in the systems such as optical parameter amplification [6,7], optical communication [25–30], etc. In fact, the in-band ASE around 980 nm can be observed in some of the literatures, such as Refs. [17,21,31], but little attention has been paid to it. In 2016, based on experimental observation, Ref. [22] called for the in-band ASE to be paid attention to in the high-power Yb-doped fiber amplifier near 980 nm, but no study was carried out on this. Later, in 2019, Ref. [32] revealed that the in-band ASE should be induced by inhomogeneous spectral broadening around 980 nm. In the same year, by studying the small-signal amplification near 976 nm in the double-cladding Yb-doped fiber, Ref. [23] revealed that the in-band ASE should be weaker than the ASE around 1030 nm and can be lowered by increasing the seed power. In 2021, Refs. [19,20] revealed that the in-band ASE can be too strong to be well suppressed in the 500-W and kW-level fiber amplifier near 980 nm. However, although recent studies made the in-band ASE more notable, there has still been no systematic study carried out on it, to the best of our knowledge.

Thus, in this paper, the in-band ASE is experimentally studied with a core-pumped single-mode Yb-doped fiber amplifier near 980 nm. It is found that the in-band ASE can still be present with the ASE around 1030 nm sufficiently suppressed. The effects of seed power, pump power, and active fiber length on the in-band ASE are also investigated in the experiment. Furthermore, in order to understand the difference between the 980-nm and 1030-nm ASEs, a theoretical study is also made.

2. Experimental Setup

The experimental setup is shown in Figure 1. Here, the single-mode Yb-doped fiber is utilized as the active fiber (providing the gain for amplification) in order for all the emissions to be operated in the fundamental mode, which can exclude the effect of transverse-mode gain competition on the in-band ASE [33]. The core diameter is about 6 μm and the cutoff wavelength is around 825 nm, which can ensure that all the emissions generated in the active fiber are single-mode. The active fiber is single-clad, and core-pumped with the laser diode (LD). Here, the core-pumping scheme is used with the consideration of suppressing the ASE around 1030 nm with sufficient pump absorption. It should be noted that the core-pumping scheme can ensure the largest core-to-cladding ratio (equal to one), which is most beneficial to the suppression of 1030-nm ASE. The peak core absorption of the Yb-doped fiber is about 26 dB/m at 915 nm.

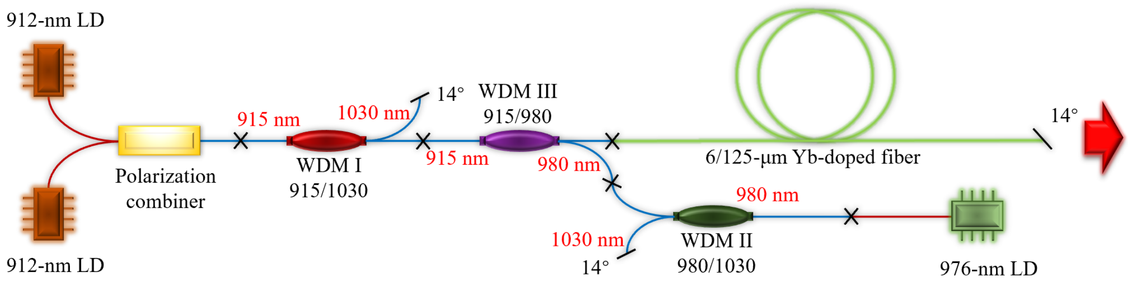

Figure 1. The experimental setup.

The pump light is provided by two laser diodes (LDs) pig-tailed with the polarization-maintaining single-mode fiber. The central wavelengths of two pump LDs are located around 912.2 nm and 911.6 nm with the 20-dB bandwidths of about 1.2 nm and 1 nm, respectively. Two pump light beams are combined and coupled into one single-mode passive fiber (for delivering the light and emission with no Yb-ion doped) through a polarization combiner, with the operating wavelength range from 905 nm to 925 nm and the insertion loss of two pump ports of 0.46 dB and 0.64 dB, respectively. The seed light is provided with a single-mode pig-tailed LD operated at 976.5 nm. Such a seed wavelength is adopted because it is the typical one within the band near 980 nm and attractive in the application of pumping Yb-doped fiber lasers and amplifiers [14–16,23,24,34]. The signal and pump light are coupled into the core of the active fiber with a 915-nm/980-nm wavelength division multiplexer (WDM, i.e., WDM III in Figure 1). The pass band of WDM III is from 910 nm to 920 nm with insertion loss of 0.59 dB, while the reflection band is from 975 nm to 985 nm with insertion loss of 0.36 dB. Then, about 160-mW seed light and 392-mW pump light can be coupled into the active fiber.

The other two WDMs (i.e., WDM I and WDM II) are the 915-nm/1030-nm and 980-nm/1030-nm ones, respectively, which are used to protect the pump LDs and seed source by filtering out the counter-propagating ASE around 1030 nm. The WDM I has a pass band from 905 nm to 925 nm with 0.3-dB insertion loss, and the WDM II has a pass band from 960 nm to 990 nm with 0.27-dB insertion loss. Both of the two WDMs have reflection bands from 1020 nm to 1080 nm with insertion loss of 0.29 dB and 0.49 dB, respectively. The unoccupied port of the active fiber is used as the output port which is angle-cleaved to suppress the optical feedback. All the passive fibers used in the experiment are adopted to match the active fiber.

3. Experimental Results

3.1. Effect of Pump Power

Firstly, the variation of the spectra with the pump power was measured, and the pertinent results are given in Figure 2. Considering that the active fiber length should be short enough to suppress the ASE around 1030 nm, the active fiber length was adopted as 1.48 m in experiment. From Figure 2a, it can be found that no obvious ASE around 1030 nm can be observed, which means that the 1030-nm ASE should be well suppressed with a 1.48-m active fiber. In spite of that, in Figure 2, the in-band ASE can be observed with a band from 972 nm to 983 nm, which means that the strong in-band ASE can be presented even with the 1030-nm ASE well suppressed. The observation also implied that the suppression of in-band ASE should be more difficult than that of 1030-nm ASE.

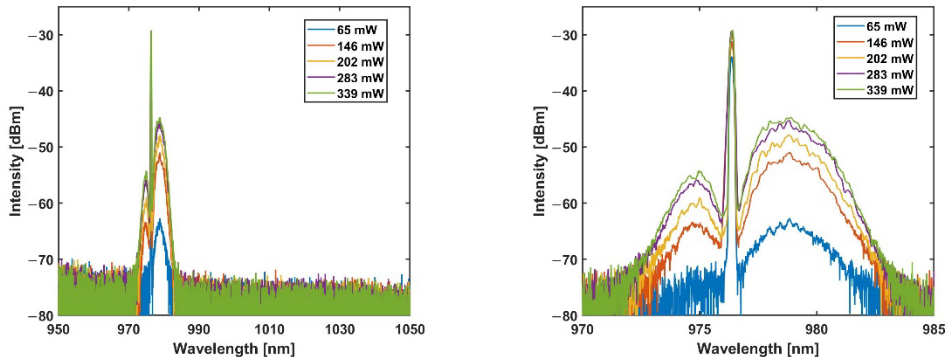

(**a**) (**b**)

Figure 2. The variation of spectra with pump power. (**b**) The zoom-in spectra of (**a**). The seed power is 41 mW.

Then, we examined the zoom-in spectra of in-band ASE, which are given in Figure 2b. It can be found that the seed light is located around 976.5 nm with a 3-dB bandwidth of 0.14 nm. Although the spectral profile of the seed light is not so stable, its central wavelength and bandwidth is not changed too much with the increment of pump power. From Figure 2b, it can also be seen that the in-band ASE is divided into two lobes because of the spectral hole-burning effect (i.e., the decrement of spectral intensity of in-band ASE around the signal light because of the gain competition between the in-band ASE and signal light) induced by the signal light [32]. In spite of that, it can be found that the peak wavelength of in-band ASE should be around 978.8 nm, which is also coincident with the spectrum of 980-nm ASE reported in Refs. [31,35–38].

From Figure 2b, it can also be seen that both the signal light and in-band ASE increase monotonously with the increment of pump power, which means that the in-band ASE cannot be well suppressed by the seed light (about 41 mW in the experiment). In order to reveal the enhancement of in-band ASE with the pump power, we calculated the power ratio of the in-band ASE to the signal light by means of spectral integration. The pertinent results are given in Figure 3. It can be found that the ratio increases monotonously with the increment of pump power, which means that the enhancement of in-band ASE is even faster than the signal light. Thus, the in-band ASE should be more dominant in the gain competition with the signal light in the fiber amplifier.

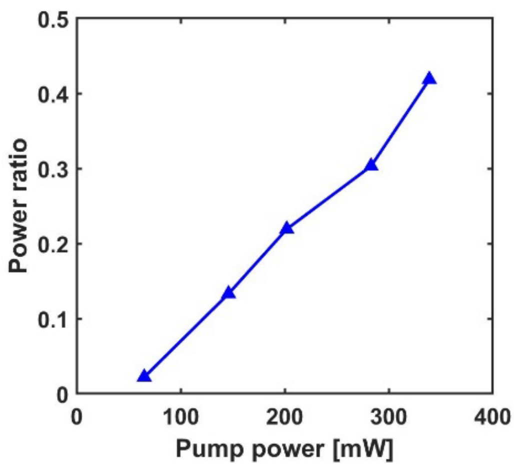

Figure 3. The variation of the power ratio of in-band ASE to signal power with the pump power. The seed power is 41 mW. The in-band ASE is calculated within the ranges of 972~975.89 nm and 976.67~983 nm, and the signal power is calculated within the range of 975.89~976.67 nm.

3.2. Effect of Seed Power

Considering the effect of seed power (i.e., the power of seed light launched into the Yb-doped fiber) in the gain competition, we then examined the effect of seed power. The results are given in Figure 4. It can be found that the whole profile of in-band ASE becomes lowered with the increment of seed power. It means that the increment of seed power is beneficial to the suppression of in-band ASE. The conclusion can also be verified by the power ratio variation given in Figure 5. It can be found that with the increment of seed power, the ratio also becomes lowered which means that the suppression of in-band ASE becomes better.

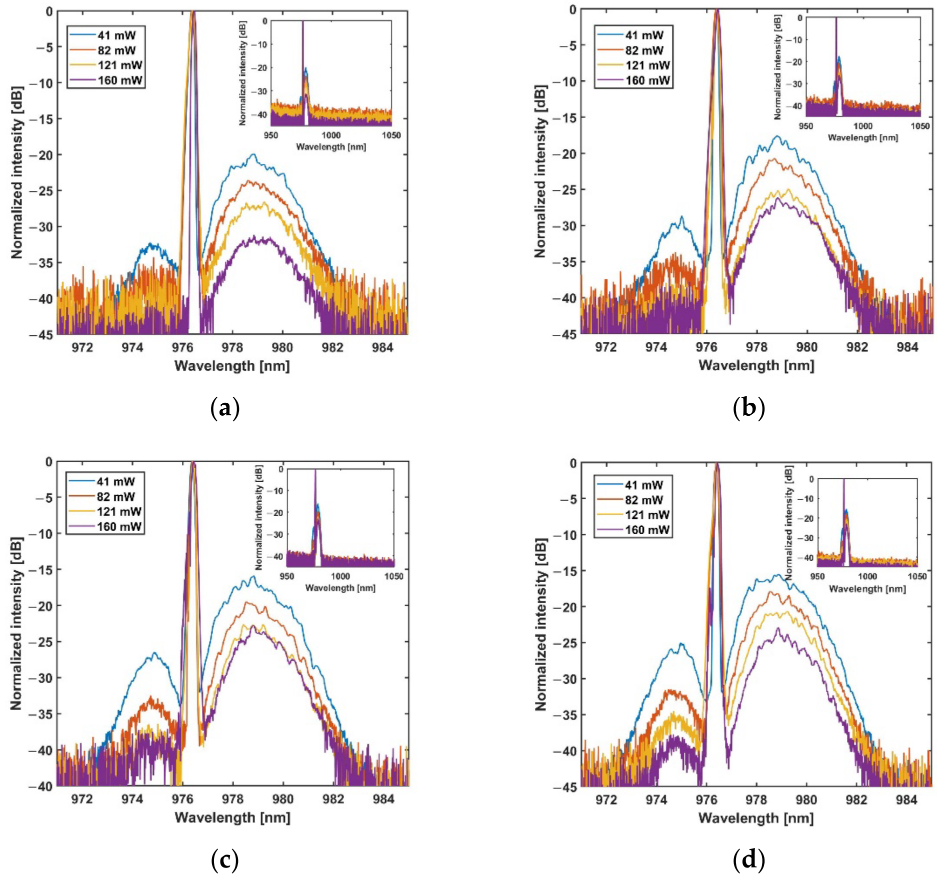

(a) (b) (c) (d)

Figure 4. The variation of spectra with seed power. Pump power: (**a**) 146 mW; (**b**) 202 mW; (**c**) 283 mW; (**d**) 339 mW. The noise in these figures is induced by the unavoidable background noise in the measurement with intensity lower than −70 dBm (see also Figure 2b).

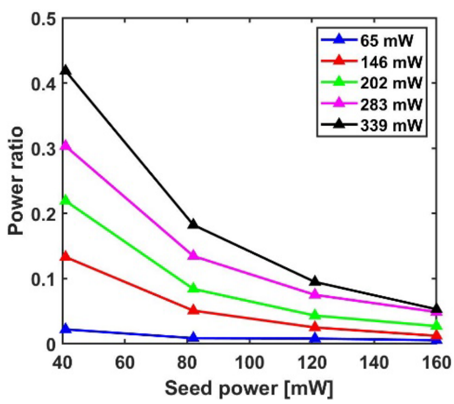

Figure 5. The variation of the power ratio of in-band ASE to signal power with the seed power.

These results can be understood with reference to the gain competition between the seed light and in-band ASE. With the increment of seed power, the seed light with larger power will consume more upper-level Yb-ions in its amplification, and then less upper-level Yb-ions are left for the amplification of in-band ASE. Thus, the signal light with larger power can be more dominant in the gain competition and the in-band ASE can be better suppressed, although the gain within the band around 980 nm is inhomogeneously broadened [32].

Furthermore, Figure 5 shows that with the increment of pump power, the reduction of the power ratio of in-band ASE becomes more rapid, which means that the effect of seed power on the in-band ASE suppression should be more effective with the larger pump power. From Figure 5, it can also be found that more seed power is needed to suppress the in-band ASE with the larger pump power, which is understandable because the stronger in-band ASE can be produced by the larger pump power (see Figure 2b). Then, more seed power is needed to suppress it. Additionally, it can also be seen that with the increment of seed power, the reduction of the power ratio becomes slower, which implies that the improvement of in-band ASE suppression becomes weaker. Especially when the pump power is lowered to 65 mW, the improvement of in-band ASE suppression is very weak (staying around 0.8%) with seed power larger than 82 mW. It means that although the in-band ASE can be better suppressed, it cannot be totally eliminated by increasing the seed power.

The variations in output powers (estimated by the spectral integration) with various seed powers are also given in Figure 6. Here, two sorts of output powers are considered, i.e., the output signal power and the total output power of signal light and in-band ASE. It can be found that both of two output powers increase linearly with the pump power, which means that the signal amplification should be in the saturation regime. It can also be found that, with the increment of seed power, the output slope efficiency (no matter the total output power or the signal power) is enlarged. This result can be understood as the larger seed power being more dominant in the gain competition, and thus, being able to obtain more gain for amplification, which makes the slope efficiency increased.

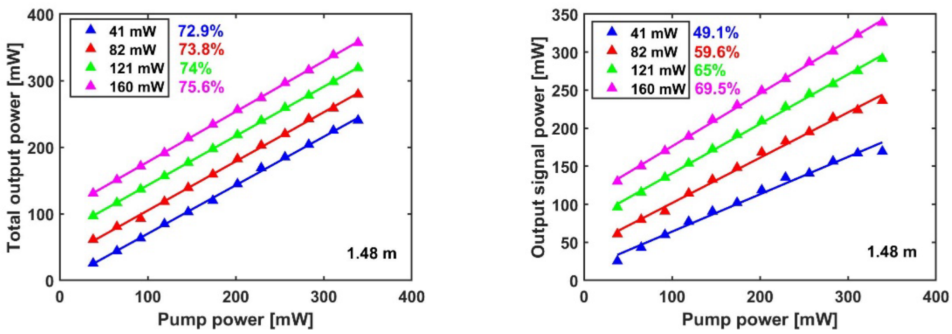

(**a**) (**b**)

Figure 6. The variation of (**a**) total output power and (**b**) output signal power with pump power. Pump thresholds with seed powers from 41 mW to 160 mW: 53.2 mW; 67.2 mW; 69.8 mW; 76.8 mW.

3.3. Effect of Active Fiber Length

Lastly, we examined the effect of the active fiber length. The pertinent results are given in Figure 7. It can be found that with each active fiber length, the power ratio of in-band ASE obeys a similar trend of variations with the seed and pump powers as mentioned above. The difference is only that the power ratio of in-band ASE is generally increased with the lengthening of the active fiber (see Figure 8). This result can be expected because the longer active fiber can absorb more pump light and then provide more gain. As a result, the in-band ASE can obtain more gain, which increases its power ratio. Thus, together with the effect of pump power discussed above, it can be concluded that with the increment in the gain of the active fiber, the power ratio of in-band ASE will be enlarged, which implies that the increment in in-band ASE power is faster than that of signal power.

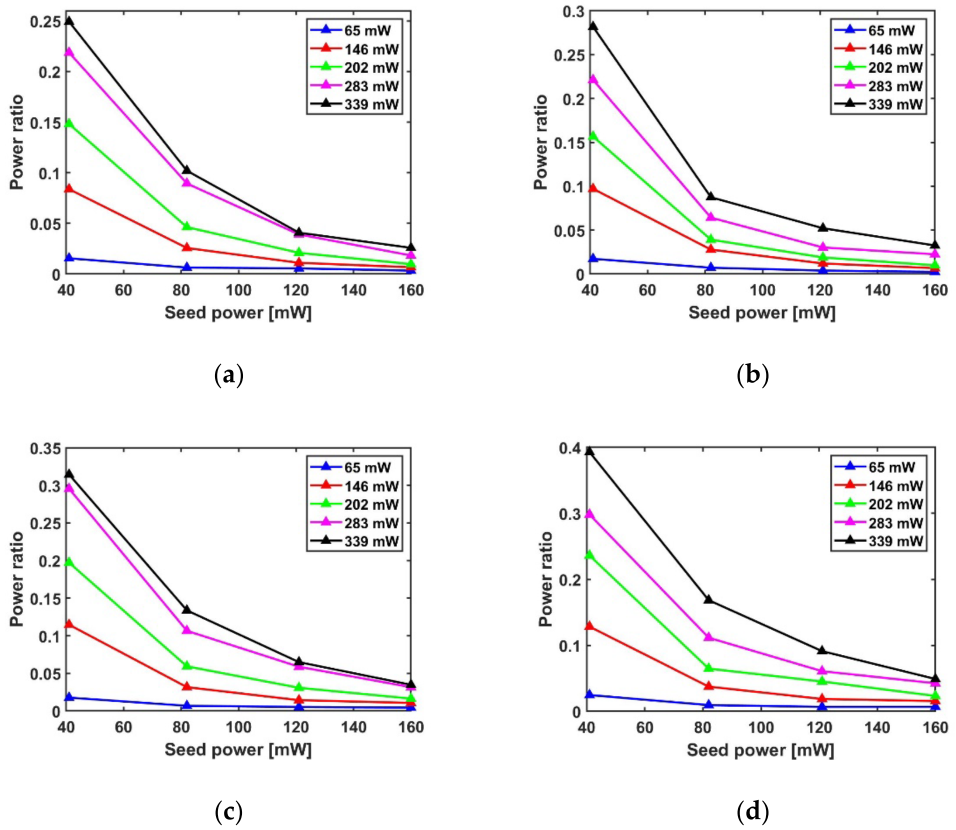

Figure 7. The variation in the power ratio of in-band ASE to signal power with the seed power corresponding to various active fiber lengths. Active fiber length: (**a**) 1.1 m; (**b**) 1.2 m; (**c**) 1.3 m; (**d**) 1.4 m.

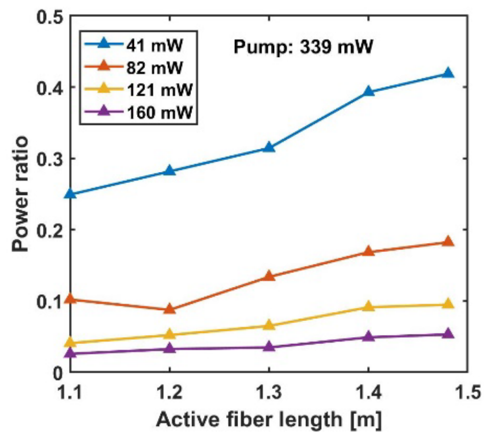

Figure 8. The variation in power ratio with active fiber length.

On another view, from Figures 7 and 8, it can also be concluded that shortening the active fiber length makes the power ratio of in-band ASE lower, which should be beneficial to the suppression of in-band ASE. However, by comparing the four figures in Figure 7, it can also be found that such improvement is very limited. Then, considering the reduction in pump absorption induced by the active fiber shortening, which will lower the pump efficiency of the fiber amplifier, shortening the active fiber is not an effective way to suppress the in-band ASE in the fiber amplifier.

The variations in output powers with 1.1-m and 1.3-m active fibers are also given in Figure 9. Together with Figure 6, it can also be found that the slope efficiency of the total output power is lowered to some extent with the active fiber length shortening because of the reduction of pump absorption. However, such lowering is only smaller than 9.7% when the active fiber length shortened from 1.48 m to 1.1 m. The reason for this is that the pump absorption (26 dB/m at 915 nm) of the Yb-doped fiber (with core-pumping scheme) is large enough to make the 1.1-m active fiber able to provide the sufficient gain for the amplification of signal light and in-band ASE. In fact, it can be found that the pump threshold is smaller than 76.8 mW even with the 1.48-m active fiber, which means that the signal amplification should be in the saturation regime. In spite of that, it can also be found that the slope efficiency of signal power is not changed so much with the lengthening of the active fiber (around 1.28%). The result is also consonant with the consideration of the enhancement of in-band ASE with the lengthening of the active fiber discussed above.

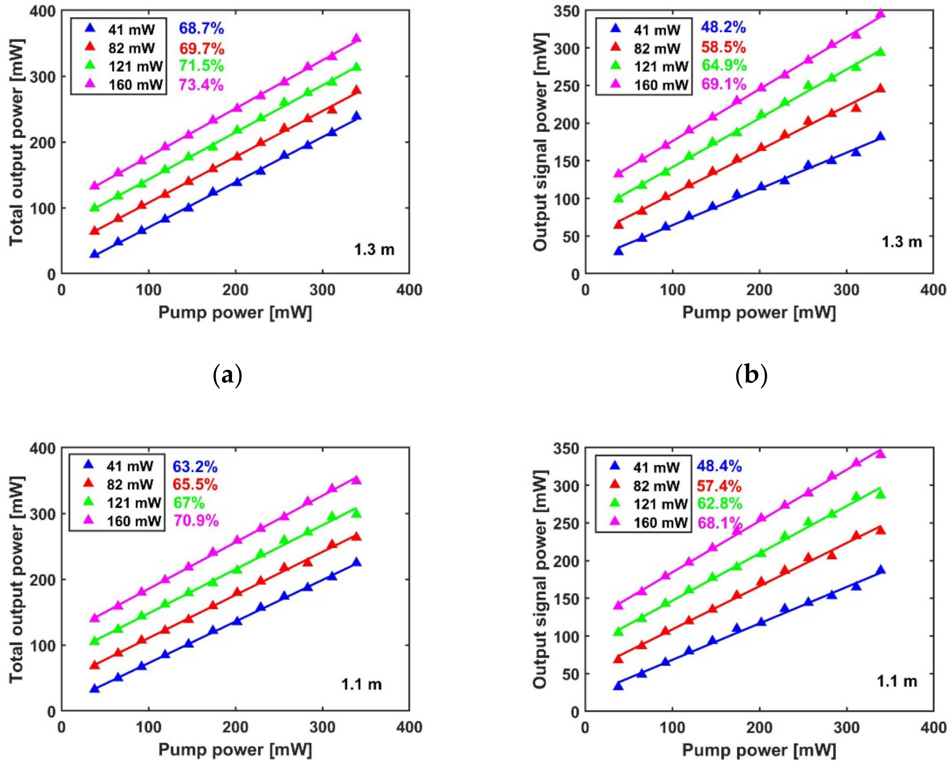

(**a**) (**b**) (**c**) (**d**)

Figure 9. The variation in output power and signal power with pump power. Active fiber length: (**a**,**b**) 1.3 m; (**c**,**d**) 1.1 m. Pump thresholds with seed powers from 41 mW to 160 mW: 1.3 m: (51.4 mW; 59.7 mW; 68.4 mW; 76.7 mW); 1.1 m: (43.6 mW; 53.4 mW; 58.9 mW; 64.1 mW).

4. Comparison with the ASE around 1030 nm

From the above discussions, it can be found that the in-band ASE around 980 nm is different from the ASE around 1030 nm, and that the suppression of in-band ASE is more difficult. However, the pertinent reason is still not so clear. In order to reveal the reason, the gains of two ASEs will be theoretically studied in this section.

According to Ref. [8], the gain of ASE can be approximated by the gain of its central wavelength G_{ASE}, which can be the function of the gain of signal light G_s and absorption of pump light α_p, and can be given as:

$$G_{ASE} = C_1\, G_s – C_2 \beta \alpha_p, \tag{1}$$

where the coefficients C_1 and C_2 are determined by the absorption and emission cross sections (represented by σ_a and σ_e, respectively) at the central wavelengths of the signal light, pump light, and ASE, and can be given as:

$$C_1 = \left(\sigma_e^{ASE}/\sigma_e^p - \sigma_a^{ASE}/\sigma_a^p\right)/\left(\sigma_e^s/\sigma_e^p - \sigma_a^s/\sigma_a^p\right), \tag{2}$$

$$C_2 = \left(\sigma_e^{ASE}/\sigma_e^s - \sigma_a^{ASE}/\sigma_a^s\right)/\left(\sigma_e^p/\sigma_e^s - \sigma_a^p/\sigma_a^s\right), \tag{3}$$

where β is approximately equal to the area ratio of inner cladding to core. Because the active fiber is single-mode and core-pumped in our experiment, the value of β should be about 1. Then, with the cross sections of Yb-doped fiber given in Ref. [39], we can obtain:

$$G_{ASE}^{979} = 0.93G_s^{976} + 0.34\beta\alpha_{912}, \tag{4}$$

$$G_{ASE}^{1030} = 0.26G_s^{976} + 0.71\beta\alpha_{912}. \tag{5}$$

Here, the cross-section values given in Ref. [39] are used in our calculation because with these values, the numerical prediction of the profile of in-band ASE (e.g., the peak wavelength around 979 nm) given in Refs. [10,11,37] agree well with our experimental observation (see Figures 2 and 4). It should be noted that the values of the cross section are related to the core matrix (e.g., the phosphate fiber [15] or phosphosilicate fiber [40]). Then, the values of coefficients C_1 and C_2 will also be changed with a different core matrix. In spite of that, the Formulas (2) and (3) should be applicable as long as the values of the cross sections obtained accord to the core matrix of the active fiber.

By comparing the two formulas, some conclusions can be drawn. The first is that both gains of the two ASE (represented by G^{979} and G^{1030}, respectively) vary monotonously with the absorption of the pump light (see the second term). It should be noted that with a given dopant concentration, the pump absorption is determined by the length of the active fiber. This can be applied to understand the experimental observation that the in-band ASE is weakened with the shorter active fiber. In spite of this, the variation of G^{1030} with the pump absorption should be faster than that of G^{979} (because the coefficient value 0.71 is larger). Thus, the gain of ASE around 1030 nm should be more sensitive to the active fiber length than that of the in-band ASE. From Equations (4) and (5), it can also be found that the effect of β (or the area ratio of inner cladding to core) is also related to the coefficient value of C_2. Therefore, the gain of ASE around 1030 nm should also be more sensitive to the core-to-cladding area ratio than that of the in-band ASE. In other words, optimizing the length and core-to-cladding ratio of the active fiber is more effective in suppressing the ASE around 1030 nm.

The second conclusion is that with the increment in signal gain (i.e., G^{976}), the increments of both G^{979} and G^{1030} are slower than that of G^{976} (because the two coefficients of the first terms in Equations (4)–(5) are smaller than 1), which implies that the signal gain G^{976} can exceed G^{979} and G^{1030} as long as the pump power is large enough. However, Equations (4)–(5) also show that to exceed G^{979} and G^{1030}, the signal gain G^{976} should be larger than $4.86\beta\alpha_{912}$ and $0.96\beta\alpha_{912}$, respectively, which means that much more pump power would be needed to exceed G^{979}. This theoretical result can be applied to understand our experimental observation that the in-band ASE grows faster than the signal light with the increment in pump power. The reason is that the pump power is not large enough to suppress the in-band ASE. Moreover, together with the less effectiveness of active fiber optimization mentioned above, it is also implied that the suppression of in-band ASE is much more difficult than that of the ASE around 1030 nm, which is the reason why the strong in-band ASE can be observed with the ASE around 1030 nm well suppressed in our experiment.

From Equation (4), it can be found that the gain G^{979} can be enhanced by enlarging the value of β, which means that the gain of in-band ASE will be increased by reducing the core-to-cladding ratio. Therefore, increasing the core-to-cladding ratio is also beneficial to the suppression of in-band ASE. Additionally, the signal gain threshold for suppressing the in-band ASE (i.e., $4.86\beta\alpha_{912}$) will also be increased by enlarging β or reducing the core-to-cladding ratio. Thus, it can be known that compared with the core-pumping scheme, the suppression of in-band ASE would be more difficult in the case of double-cladding fiber with the cladding-pumping scheme. Although Equation (4) also shows that the gain of in-band ASE can be lowered by reducing the pump absorption (i.e., α_{912}), such a method will also lower the pump efficiency of the fiber amplifier. Therefore, the question of how to suppress the in-band ASE in the double-cladding Yb-doped fiber amplifier still needs further investigation.

Lastly, it should be noted that the above discussions relate to a signal light of around 976 nm. If the signal wavelength varies, the profile of in-band ASE (e.g., the peak wavelength and bandwidth) will also be varied correspondingly [11,31]. In spite of this, the method of theoretical analysis presented above can also be applied for other signal wavelengths within the band near 980 nm, as long as the ASE wavelength and pertinent parameter values can be adopted according the profile of in-band ASE.

5. Conclusions

In conclusion, the in-band ASE around 980 nm is experimentally studied with a core-pumped single-mode Yb-doped fiber amplifier for the first time, to the best of our knowledge. The effects of pump power, seed power, and active fiber length on the in-band ASE are investigated. It is found, unexpectedly to some extent, that the strong in-band ASE around 980 nm can be present even with the ASE around 1030 nm well suppressed, and its enhancement is faster than the signal light with an increment in pump power. It is also found that the in-band ASE can be weakened by increasing the seed power and shortening the active fiber. However, the results imply that increasing the seed power should be more effective in suppressing the in-band ASE, and more seed power is needed with the increment in pump power. In comparison, shortening the active fiber is not so effective at suppressing the in-band ASE, which is very different from the case of the ASE around 1030 nm, which can be effectively suppressed by shorting the active fiber [8–10,37].

Furthermore, in order to better understand the difference between two ASEs, their gains are theoretically analyzed with the gain competition theory given in Ref. [8]. It is revealed that the suppression of in-band ASE is more difficult than that of the 1030-nm ASE, which may also be the reason for the presence of the strong in-band ASE reported in Refs. [19,20]. It is also implied that the in-band ASE will play a very important role in the high-power Yb-doped fiber amplifier operating near 980 nm. Our study presented in this paper should provide significant guidance for understanding the in-band ASE in the high-power Yb-doped fiber amplifier near 980 nm and can also provide guidance on the designation of systems involving the Yb-doped fiber amplifiers.

Author Contributions: Methodology, J.C. (Jianqiu Cao); validation, J.C. (Jianqiu Cao); formal analysis, Z.L. and S.Z.; investigation, Z.L., S.Z., A.L. and Z.H.; resources, J.C. (Jianqiu Cao); data curation, Z.L., S.Z. and A.L.; writing—original draft preparation, Z.L. and S.Z.; writing—review and editing, J.C. (Jianqiu Cao) and Z.H.; visualization, Z.L. and S.Z.; supervision, J.C. (Jianqiu Cao) and J.C. (Jinbao Chen); project administration, J.C. (Jianqiu Cao) and J.C. (Jinbao Chen); funding acquisition, J.C. (Jinbao Chen). All authors have read and agreed to the published version of the manuscript.

Funding: This research received no external funding.

Institutional Review Board Statement: Not applicable.

Informed Consent Statement: Not applicable.

Data Availability Statement: Data underlying the results presented in this paper are not publicly available at this time but may be obtained from the authors upon reasonable request.

Conflicts of Interest: The authors declare no conflict of interest.

References

1. Tünnermann, A.; Schreiber, T.; Limpert, J. Fiber lasers and amplifiers: An ultrafast performance evolution. *Appl. Opt.* **2010**, *49*, F71–F78. [CrossRef] [PubMed]
2. Zervas, M.N.; Codemard, C.A. High Power Fiber Lasers: A Review. *IEEE J. Sel. Top. Quantum Electron.* **2014**, *20*, 219–241. [CrossRef]
3. Kurkov, A.S. Oscillation spectral range of Yb-doped fiber lasers. *Laser Phys. Lett.* **2007**, *4*, 93–102. [CrossRef]
4. Richardson, D.J.; Nilsson, J.; Clarkson, W.A. High power fiber lasers: Current status and future perspectives [Invited]. *J. Opt. Soc. Am. B* **2010**, *27*, B63–B92. [CrossRef]
5. Shiner, B. The Impact of Fiber Laser Technology on the World Wide Material Processing Market. In Proceedings of the CLEO: Applications and Technology 2013, San Jose, CA, USA, 9–14 June 2013.
6. Soh, D.B.S.; Codemard, C.; Wang, S.; Nilsson, J.; Sahu, J.; Laurell, F.; Philippov, V.; Jeong, Y.; Alegria, C.; Baek, S. A 980-nm Yb-Doped Fiber MOPA Source and Its Frequency Doubling. *IEEE Photonics Technol. Lett.* **2004**, *16*, 1032–1034. [CrossRef]
7. Laroche, M.; Bartolacci, C.; Cadier, B.; Gilles, H.; Girard, S.; Lablonde, L.; Robin, T. Generation of 520 mW pulsed blue light by frequency doubling of an all-fiberized 978 nm Yb-doped fiber laser source. *Opt. Lett.* **2011**, *36*, 3909–3911. [CrossRef]
8. Nilsson, J.; Minelly, J.D.; Paschotta, R.; Tropper, A.C.; Hanna, D.C. Ring-doped cladding-pumped single-mode three-level fiber laser. *Opt. Lett.* **1998**, *23*, 355–357. [CrossRef]
9. Wang, R.; Liu, Y.; Cao, J.; Guo, S.; Si, L.; Chen, J. Experimental study on the all-fiberized continuous-wave ytterbium-doped laser operating near 980 nm. *Appl. Opt.* **2013**, *52*, 5920–5924. [CrossRef]
10. Liu, Y.; Cao, J.; Xiao, H.; Guo, S.; Si, L.; Huang, L. Study on the output properties of fiber lasers operating near 980 nm. *J. Opt. Soc. Am. B* **2013**, *30*, 266. [CrossRef]
11. Ren, Y.; Cao, J.; Du, S.; Chen, J. Numerical study on the continuous-wave Yb-doped fiber amplifiers operating near 980 nm. *Optik* **2018**, *161*, 118–128. [CrossRef]
12. Boullet, J.; Zaouter, Y.; Desmarchelier, R.; Cazaux, M.; Salin, F.; Saby, J.; Bello-Doua, R.; Cormier, E. High power ytterbium-doped rod-type three-level photonic crystal fiber laser. *Opt. Express* **2008**, *16*, 17891–17902. [CrossRef] [PubMed]
13. Li, W.; Matniyaz, T.; Gafsi, S.; Kalichevsky-Dong, M.T.; Hawkins, T.W.; Parsons, J.; Gu, G.; Dong, L. 151W monolithic diffraction-limited Yb-doped photonic bandgap fiber laser at similar to 978nm. *Opt. Express* **2019**, *27*, 24972–24977. [CrossRef] [PubMed]
14. Aleshkina, S.S.; Bardina, T.L.; Lipatov, D.S.; Bobkov, K.K.; Bubnov, M.M.; Gur'yanov, A.N.; Likhachev, M.E. Factors reducing the efficiency of ytterbium fibre lasers and amplifiers operating near 0.98 μm. *Quantum Electron.* **2017**, *47*, 1109. [CrossRef]
15. Wu, J.; Zhu, X.; Temyanko, V.; LaComb, L.; Kotov, L.; Kiersma, K.; Zong, J.; Li, M.; Chavez-Pirson, A.; Norwood, R.A.; et al. Yb^{3+}-doped double-clad phosphate fiber for 976 nm single-frequency laser amplifiers. *Opt. Mater. Express* **2017**, *7*, 1310. [CrossRef]
16. Valero, N.; Feral, C.; Lhermite, J.; Petit, S.; Royon, R.; Bardin, Y.-V.; Goeppner, M.; Dixneuf, C.; Guiraud, G.; Proulx, M.A.; et al. 39 W narrow spectral linewidth monolithic ytterbium-doped fiber MOPA system operating at 976 nm. *Opt. Lett.* **2020**, *45*, 1495–1498. [CrossRef]
17. Soh, D.B.S.; Codemard, C.; Sahu, J.K.; Nilsson, J.; Philippov, V.; Alegria, C.; Jeong, Y. A 4.3 W 977 nm Ytterbium-doped Jacketed-Air-Clad Fiber Amplifier. In Proceedings of the Advanced Solid-State Photonics 2004, Santa Fe, NM, USA, 1–4 February 2004. [CrossRef]
18. Kim, J.P.; Park, J.S.; Oh, Y.J.; Han, E.H.; Park, E.J.; Jeong, H.; Jung, Y.; Lee, K.; Lee, Y.; Cho, J. High-power extra-large-mode-area Yb-doped fiber laser and amplifier at 978 nm. *J. Korean Phys. Soc.* **2021**, *78*, 1062–1066. [CrossRef]
19. Chen, M.; Cao, J.; Liu, A.; Huang, Z.; Pan, Z.; Chen, Z.; Chen, J. Demonstration of kilowatt monolithic Yb-doped fiber laser operation near 980 nm. *Opt. Lett.* **2021**, *46*, 5340. [CrossRef]
20. Chen, M.; Cao, J.; Liu, A.; Huang, Z.; Pan, Z.; Chen, Z.; Chen, J. Experimental study on the 500-W-level all-fiber amplifier operating near 980 nm. *Results Phys.* **2021**, *29*, 104784. [CrossRef]
21. Aleshkina, S.S.; Likhachev, M.E.; Lipatov, D.S.; Medvedkov, O.I.; Bobkov, K.K.; Bubnov, M.M.; Guryanov, A.N. 5.5 W monolitic single-mode fiber laser and amplifier operating near 976 nm. *Fiber Lasers XIII: Technol. Syst. Appl.* **2016**, *9728*, 265–272. [CrossRef]
22. Yu, Y.; An, Y.; Cao, J.; Guo, S.; Xu, X. Experimental Study on All-Fiberized Continuous-Wave Yb-Doped Fiber Amplifier Operating Near 980 nm. *IEEE Photonics Technol. Lett.* **2015**, *28*, 398–401. [CrossRef]
23. Aleshkina, S.S.; Lipatov, D.S.; Kochergina, T.A.; Velmiskin, V.V.; Temyanko, V.L.; Kotov, L.V.; Bardina, T.L.; Bubnov, M.M.; Guryanov, A.N.; Likhachev, M.E. All-fibre single-mode small-signal amplifier operating near 0.976 μm. *Quantum Electron.* **2019**, *49*, 919–924. [CrossRef]
24. Kotov, L.; Temyanko, V.; Aleshkina, S.; Bubnov, M.; Lipatov, D.; Likhachev, M. Efficient single-mode 976 nm amplifier based on a 45 micron outer diameter Yb-doped fiber. *Opt. Lett.* **2020**, *45*, 4292. [CrossRef] [PubMed]
25. Jin, C.; Shevchenko, N.A.; Li, Z.; Popov, S.; Chen, Y.; Xu, T. Nonlinear Coherent Optical Systems in the Presence of Equalization Enhanced Phase Noise. *J. Lightwave Technol.* **2021**, *39*, 4646–4653. [CrossRef]
26. You, Y.; Shen, H.; Qi, Y.; He, B.; Zhou, J. Low-noise frequency and phase locking of Yb-doped fiber ring cavity via cavity modulation. *J. Lightwave Technol.* **2022**. [CrossRef]
27. Bui, T.N.; Nguyen, Q.T.; Pham, V.H. Influence of ASE Noise on the Performance of DWDM Networks Using Low-Power Pumped Raman Amplifiers. *IETE J. Res.* **2015**, *62*, 239–245. [CrossRef]
28. Huang, J. Impact of ASE noise in WDM systems. *Optik* **2011**, *122*, 1376–1380. [CrossRef]

29. Hiçdurmaz, B.; Temurtaş, H.; Karlık, S.E.; Yılmaz, G. A novel method degrading the combined effect of FWM and ASE noise in WDM systems containing in-line optical amplifiers. *Optik* **2013**, *124*, 4064–4071. [CrossRef]
30. Tithi, F.H.; Majumder, S.P. Combined Effect of ASE Noise and SRS Induced Crosstalk on the BER Performance of a Single Span WDM System with Raman Amplifier Using Heterodyne Coherent Detection. *J. Opt. Commun.* **2020**, *41*, 347–354. [CrossRef]
31. Jelger, P.; Engholm, M.; Norin, L.; Laurell, F. Degradation-resistant lasing at 980 nm in a Yb/Ce/Al-doped silica fiber. *J. Opt. Soc. Am. B* **2010**, *27*, 338–342. [CrossRef]
32. Matniyaz, T.; Li, W.; Kalichevsky-Dong, M.; Hawkins, T.W.; Parsons, J.; Gu, G.; Dong, L. Highly efficient cladding-pumped single-mode three-level Yb all-solid photonic bandgap fiber lasers. *Opt. Lett.* **2019**, *44*, 807–810. [CrossRef]
33. Jiang, Z.; Marciante, J.R. Impact of transverse spatial-hole burning on beam quality in large-mode-area Yb-doped fibers. *J. Opt. Soc. Am. B* **2008**, *25*, 247–254. [CrossRef]
34. Leich, M.; Jäger, M.; Grimm, S.; Hoh, D.; Jetschke, S.; Becker, M.; Hartung, A.; Bartelt, H. Tapered large-core 976 nm Yb-doped fiber laser with 10 W output power. *Laser Phys. Lett.* **2014**, *11*, 045102. [CrossRef]
35. Ren, Y.; Cao, J.; Ying, H.; Chen, H.; Pan, Z.; Du, S.; Chen, J. Demonstration of multi-Watt all-fiber superfluorescent source operating near 980 nm. *Chin. Phys. B* **2018**, *27*, 030703. [CrossRef]
36. Ren, Y.; Cao, J.; Ying, H.; Chen, H.; Pan, Z.; Du, S.; Chen, J. Experimental study on high-power all-fiber superfluorescent source operating near 980 nm. *Laser Phys. Lett.* **2018**, *15*, 075105. [CrossRef]
37. Ren, Y.; Cao, J.; Chen, H.; Ying, H.; Pan, Z.; Du, S.; Chen, J. Study on the power scalability of all-fiber superfluorescent source operating near 980 nm. *Opt. Express* **2018**, *26*, 17830–17840. [CrossRef]
38. Du, H.; Cao, J.; Liu, A.; Pan, Z.; Ren, Y.; Chen, H.; Huang, Z.; Chen, J. Study on improving the efficiency of superfluorescent Yb-doped fiber source operating near 980 nm with distributed side-coupled cladding-pumped fiber. *Opt. Fiber Technol.* **2019**, *53*, 101991. [CrossRef]
39. Paschotta, R.; Nilsson, J.; Barber, P.R.; Caplen, J.E.; Tropper, A.C.; Hanna, D.C. Lifetime quenching in Yb-doped fibres. *Opt. Commun.* **1997**, *136*, 375–378. [CrossRef]
40. Melkumov, M.; Bufetov, A.I.; Kravtsov, K.S.; Shubin, A.V.; Dianov, E.M. Lasing parameters of ytterbium-doped fibres doped with P_2O_5 and Al_2O_3. *Quantum Electron.* **2004**, *34*, 843–848. [CrossRef]